Journal of Sound and Vibration (1998) **216**(3), 529–538
Article No. sv981753

LETTERS TO THE EDITOR

IS A COLLOCATED PIEZOELECTRIC SENSOR/ACTUATOR PAIR FEASIBLE FOR AN INTELLIGENT BEAM?

S. Y. Yang and W. H. Huang
Department of Precision Machinery and Precision Instrumentation, University of Science and Technology of China, Hefei, Anhui, 230026, *People's Republic of China*

(*Received* 1 *September* 1997, *and in final form* 27 *April* 1998)

1. Introduction

The use of distributed piezoelectric sensors and actuators for sensing and control of the vibration of flexible structures, i.e., to construct intelligent structures, has drawn much attention during the past decade [1–3]. The collocated rectangular sensor/actuator pair technique, i.e., the sensor and the actuator of one sensor/actuator pair are located at the same position but symmetrically distributed with respect to the midplane of a structure (such as a beam, a plate of a shell, etc.), is usually used when one models and analyzes a piezoelectric intelligent structure for its simplicity [2, 4–6]. An intelligent beam with a collocated sensor/actuator pair is shown in Figure 1, which can be considered as the simple model of a piezoelectric distributed control system. The top and bottom layers of the laminated beam are made from the same piezoelectric material, such as polyvinylidene fluoride polymer (PVDF) or lead zirconate/titanate (PZT), etc. The portions covered by surface electrodes of the two piezoelectric layers serve as the sensor and actuator, respectively. The length and width of the beam are l_0 and w, respectively, and the thickness of the layers is h_1, h_2 and h_1. The left and right ends of the sensor (or actuator) are l_1 and l_2 from the clamped end of the beam,

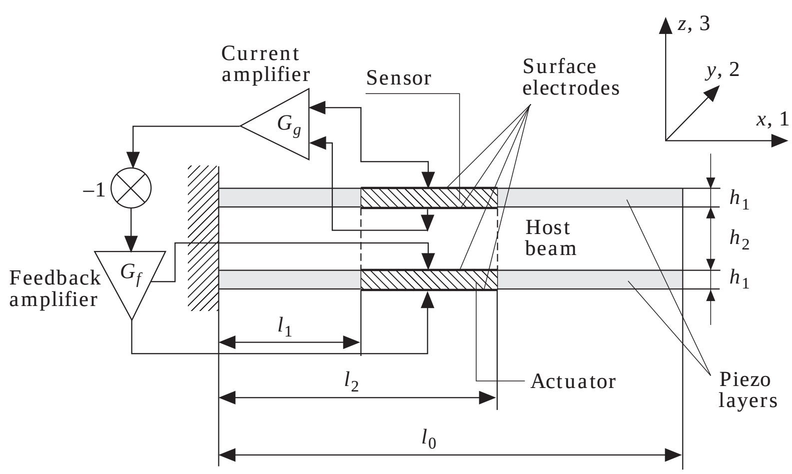

Figure 1. An intelligent beam with a collocated piezoelectric sensor/actuator pair integrated in its top and bottom layer.

0022–460X/98/380529 + 10 $30.00/0

respectively. For the piezoelectric layers and the middle (beam) layer the densities are ρ_1 and ρ_2; the Young's moduli are Y_1 and Y_2 respectively. This configuration of the sensor and actuator of the beam is convenient for integration, as was first proposed by Lee [7]. The negative feedback control method shown in Figure 1 was also proposed by Lee [8], which is really negative velocity feedback and necessary for the control of the vibration of the beam and is used widely.

Generally, the sensing effect and actuation effect of a collocated sensor/actuator pair are asymmetric with respect to the midplane of the flexible structure. The sensor of a sensor/actuator pair not only senses the transverse motion (motion in the direction in which the structure has a lower stiffness) of the structure, which is expected by the initial design, but also senses the longitudinal motion (motion in the direction in which the structure has a higher stiffness), which is not expected by the initial design. The actuation effect produced by the actuator also has a longitudinal component, which then produces longitudinal motion. In the previous related analytical and numerical analysis of the vibration suppression of a flexible structure using collated sensor/actuator(s) (more widely, using asymmetric distributed sensing and actuating techniques), only the transverse motion is considered and the longitudinal motion is neglected [4, 5, 9–12]. They all show effective vibration suppression in transverse direction by using the feedback method shown in Figure 1. In this letter, the beam shown in Figure 1 will be analyzed exactly by considering both transverse and longitudinal vibrations of the beam. Through numerical calculation, such an adaptive control method will be shown to be dispersive and will enhance the vibration of such a beam instead of suppressing it. That is, such a piezoelectric sensor/actuator pair is not feasible for an intelligent beam. In addition, the analysis method presented here will reveal directly and analytically the control (damping) effect of the sensor/actuator pair on the closed-loop motion of the beam, while the previous methods can only show this damping effect by the finite element method (FEM) [5, 13]. The present method can be used to analyze distributed piezoelectric control structures that are more complicated than the intelligent beam.

2. ANALYSIS

For the convenience of analyzing the motion of the beam, first one introduces a new analytical method, which deals with the electric excitation in a piezoelectric element as its equivalent normal actuation forces acting on the element whilst simultaneously regarding the element as a normal elastic body. As to a one-dimensional piezoelectric actuator (see Figure 2(a)), which operates in extension mode under the exciting of a voltage $V(t)$, based on the fundamental knowledge in piezoelectricity [14] one can obtain the equivalent actuation forces of the exciting voltage as the two equal and opposite forces, $F_1(t)$ and $F_2(t)$, shown in Figure 2(b), where $F_1(t) = F_2(t) = d_{31} w V(t)/s^E_{11}$, t is the time, d_{31} and s^E_{11} are the piezoelectric strain/charge constant and the elastic compliance constant of the piezoelectric material respectively. Then the dynamics of the actuator is transformed into the dynamics of the elastic body shown in Figure 2(b), whose Young's modulus is $1/s^E_{11}$.

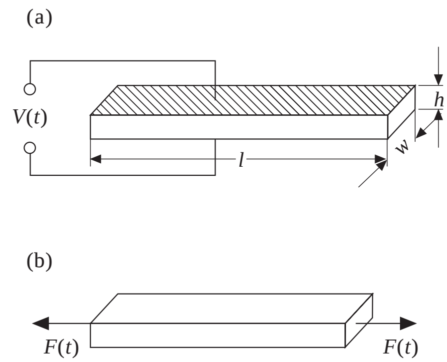

Figure 2. (a) A one-dimensional piezoelectric actuator that operates in extension mode; (b) the equivalent actuation forces of the applied voltage on the actuator shown in (a).

In Figure 1, the electric field in the sensor is zero during close-circuit operation of the sensor. All stress components, except for the longitudinal T_1, can be neglected for the one-dimensional configuration of the beam. Then in the sensor, $D_3 = d_{31}T_1$ and $S_1 = s_{11}^E T_1$, where D_3 is the electric displacement, S_1 is the longitudinal strain, and $s_{11}^E = 1/Y_1$. The displacement along the 1 (longitudinal or x) and 3 (transverse or z) directions of the midplane of the beam are marked by u_1 and u_3 respectively. The origin of the co-ordinate system is located at the center of the clamped end of the beam. According to the classical laminated plate theory, the longitudinal strain of the point, whose co-ordinate in the direction 3 is z, can be written as $S_1 = \partial u_1/\partial x - z\partial^2 u_3/\partial x^2$. The current flow from the sensor is $i_s(t) = \mathrm{d}q_s(t)/\mathrm{d}t$, where $q_s(t)$ is the charge developed by the sensor and can be written as

$$q_s(t) = 1/2\left[\int_{l_1}^{l_2} (D_3|_{z=h_2/2})w\,\mathrm{d}x + \int_{l_1}^{l_2} (D_3|_{z=(h_1+h_2)/2})w\,\mathrm{d}x\right].$$

According to the above analysis,

$$i_s(t) = d_{31}wY_1\frac{\mathrm{d}}{\mathrm{d}t}\left\{2[u_1(l_2, t) - u_1(l_1, t)] - \left(\frac{h_1}{2} + h_2\right)[u_3'(l_2) - u_3'(l_1)]\right\}, \quad (1)$$

where the superscript $'$ represents the first derivative with respect to x.

Obviously, the total feedback gain of the beam is $G = -G_f G_g$. Then the feedback voltage applied to the actuator is

$$V_a(t) = Gi_s(t). \quad (2)$$

By directly substituting the result shown in Figure 2 into the intelligent beam in Figure 1, one can obtain the two forces induced by $V_a(t)$, marked by P_1 and P_2, acting on the left and right ends of the actuator of the beam respectively. There is

$$P_1 = P_2 = P(t) = d_{31}wY_1V_a(t). \quad (3)$$

Hence, according to the knowledge in vibration dynamics [15] the equations of motion (EOM) of the beam can be written as

$$\rho A \partial^2 u_1/\partial t^2 - YA\partial^2 u_1/\partial x^2 = [-\delta(x-l_1) + \delta(x-l_2)]P(t),$$

$$\rho A \partial^2 u_3/\partial t^2 + YI\partial^4 u_3/\partial x^4 = -(\partial/\partial x)[-\delta(x-l_1) + \delta(x-l_2)]M(t), \quad \text{(4a, 4b)}$$

where $\rho A = (2\rho_1 h_1 + \rho_2 h_2)w$ is the mass density per unit length of the beam, $YA = (2Y_1 h_1 + Y_2 h_2)w$ and $YI = \{2Y_1 h_1[h_1^2/12 + (h_1 + h_2)^2/4] + Y_2 h_2^3/12\}w$ are the rigidities of the beam in the longitudinal and transverse directions respectively, $\delta(x)$ is the delta function, and $M(t) = (h_1 + h_2)P(t)/2$ is the moment of the force $P(t)$ with respect to the principal inertia axis of the cross-section of the beam. Equations (4a) and (4b) describe the motions of the beam in the longitudinal and transverse directions respectively. They can also be derived from the general EOM of laminated piezoelectric plates with the aid of the Heaviside function [6, 16]. However, the present method for the derivation of the equations is clearer and more straightforward, which is just based on the results in the well-studied classical mechanics and does not need any help of other mathematical tools.

Assuming there are no other forces acting on the beam, by substituting equations (1), (2) and (3) into equations (4a, b), one can get the closed-loop EOM of the beam:

$$\rho A \partial^2 u_1/\partial t^2 - YA\partial^2 u_1/\partial x^2 = (d_{31} w Y_1)^2 G[-\delta(x-l_1) + \delta(x-l_2)]$$
$$\times (\mathrm{d}/\mathrm{d}t)\{2[u_1(l_2, t) - u_1(l_1, t)] - (h_1/2 + h_2)[u_3'(l_2) - u_3'(l_1)]\},$$
$$\rho A \partial^2 u_3/\partial t^2 + YI\partial^4 u_3/\partial x^4 = -[(h_1 + h_2)/2](d_{31} w Y_1)^2 G(\partial/\partial x)[-\delta(x-l_1)$$
$$+ \delta(x-l_2)] \times \frac{\mathrm{d}}{\mathrm{d}t}\{2[u_1(l_2, t) - u_1(l_1, t)] - (h_1/2 + h_2)[u_3'(l_2) - u_3'(l_1)]\}.$$

(5a, b)

According to the vibration mode superposition method, u_1 and u_3 can be expressed as

$$u_1(x, t) = \sum_{i=1}^{\infty} U_{1i}(x)\eta_{1i}(t), \qquad u_3(x, t) = \sum_{i=1}^{\infty} U_{3i}(x)\eta_{3i}(t), \quad \text{(6a, b)}$$

where $U_{1i}(x)$ and $U_{3i}(x)$, $\eta_{1i}(t)$ and $\eta_{3i}(t)$ ($i = 1, 2, 3, \ldots$) are the normalized mode shapes, modal co-ordinates of the beam in the directions 1 and 3 respectively, and i is the order. Additionally, the $U_{1i}(x)$ and $U_{3i}(x)$ in equations (6a) and (6b) can be expressed as

$$U_{1i}(x) = B_{1i} \sin(i\pi x/2l_0), \quad \text{(7a)}$$

$$U_{3i}(x) = B_{3i}[\cos\beta_i x - \cosh\beta_i x + r_i \sin\beta_i x - \sinh\beta_i x)], \quad \text{(7b)}$$

respectively where $r_i = (\sin \beta_i l_0 - \sinh \beta_i l_0)/(\cos \beta_i l_0 + \cosh \beta_i l_0)$, β_i satisfies the equation $\cos \beta_i l_0 \cosh \beta_i l_0 = -1$, B_{ki} is determined by the following normalization condition

$$\int_0^{l_0} \rho A U_{ki}^2(x)\,\mathrm{d}x = 1, \qquad k = 1, 3, \qquad i = 1, 2, 3, \ldots .$$

The corresponding natural frequencies of the beam are $\omega_{1i} = (2i-1)\pi a/2l_0$, $\omega_{3i} = (\beta_i l_0)^2\sqrt{YI/\rho A l_0^4}$, where $a = \sqrt{YI/\rho A}$. By substituting equations (6a) and (6b) into equations (5a) and (5b), and multiplying equations (5a) and (5b) by $U_{1j}(x)$ and $U_{3j}(x)$, then integrating equations (5a) and (5b) along the length of the beam, and applying the orthogonalities between arbitrary two modes, one gets

$$\ddot{\eta}_{1j} + \left(b_1 \sum_{i=1}^{\infty} c_{1i}\dot{\eta}_{1i} + b_2 \sum_{i=1}^{\infty} c_{3i}\dot{\eta}_{3i}\right)c_{1j} + \omega_{1j}^2\eta_{1j} = 0, \tag{8a}$$

$$\ddot{\eta}_{3j} + \left(b_3 \sum_{i=1}^{\infty} c_{1i}\dot{\eta}_{1i} + b_4 \sum_{i=1}^{\infty} c_{3i}\dot{\eta}_{3i}\right)c_{3j} + \omega_{3j}^2\eta_{3j} = 0, \tag{8b}$$

respectively, where

$$b_1 = -2D, \qquad b_2 = (h_1/2 + h_2)D, \qquad b_3 = -(h_1 + h_2)D,$$

$$b_4 = (h_1 + h_2)(h_1 + 2h_2)D/4, \qquad D = (d_{31} w Y_1)^2 G,$$

$$c_{1i} = U_{1i}(l_2) - U_{1i}(l_1), \qquad c_{3i} = U'_{3i}(l_2) - U'_{3i}(l_1), \qquad i, j = 1, 2, 3, \ldots,$$

and the superscript $\cdot$ and $\cdot\cdot$ are the first and second order derivatives with respect to the time t. If the initial conditions of the beam are $u_1(x, 0)$, $\dot{u}_1(x, 0)$, $u_3(x, 0)$ and $\dot{u}_3(x, 0)$, the initial conditions of the modal co-ordinates can be obtained as

$$\eta_{kj}(0)\int_0^{l_0} \rho A u_k(x, 0) U_{kj}(x)\,\mathrm{d}x, \tag{9a}$$

$$\dot{\eta}_{kj}(0) = \int_0^{l_0} \rho A \dot{u}_k(x, 0) U_{kj}(x)\,\mathrm{d}x, \qquad k = 1, 3 \text{ and } j = 1, 2, 3, \ldots . \tag{9b}$$

If mode truncation is made and the former n orders of modes are adopted to analysis, equations (8a, b) have $2n$ equations that are the same in form as those governing the motion of a general damped system with $2n$ degrees. In this situation equations (8a, b) can be written as

$$\mathbf{M}\ddot{\boldsymbol{\eta}} + \mathbf{C}\dot{\boldsymbol{\eta}} + \mathbf{K}\boldsymbol{\eta} = \mathbf{0}, \tag{10}$$

where

$$\boldsymbol{\eta} = [\eta_{11}, \eta_{12}, \ldots, \eta_{1n}, \eta_{31}, \eta_{32}, \ldots, \eta_{3n}]^{\mathrm{T}},$$

$$\mathbf{M} = \mathbf{I}_{2n \times 2n}, \qquad \mathbf{K} = \operatorname{diag}\,[\omega_{11}^2 \omega_{12}^2 \cdots \omega_{1n}^2 \omega_{31}^2 \omega_{32}^2 \cdots \omega_{3n}^2],$$

and

$$\mathbf{C} = \begin{bmatrix} b_1 c_{11}^2 & b_1 c_{12} c_{11} & \cdots & b_1 c_{1n} c_{11} & b_2 c_{31} c_{11} & b_2 c_{32} c_{11} & \cdots & b_2 c_{3n} c_{11} \\ b_1 c_{11} c_{12} & b_1 c_{12}^2 & \cdots & b_1 c_{1n} c_{12} & b_2 c_{31} c_{12} & b_2 c_{32} c_{12} & \cdots & b_2 c_{3n} c_{12} \\ \vdots & \vdots & \vdots & \vdots & \vdots & \vdots & \vdots & \vdots \\ b_3 c_{11} c_{3n} & b_3 c_{12} c_{3n} & \cdots & b_3 c_{1n} c_{3n} & b_4 c_{31} c_{3n} & b_4 c_{32} c_{3n} & \cdots & b_4 c_{3n}^2 \end{bmatrix} \tag{11}$$

the superscript T denotes the transposition of a matrix, and $\mathbf{I}_{2n \times 2n}$ is the unit matrix of $2n$ order. One can use the state space method to solve equation (10). The state space variable is

$$\boldsymbol{\xi} = [\boldsymbol{\eta} \quad \dot{\boldsymbol{\eta}}]^{\mathrm{T}}. \tag{12}$$

The state space equation of the $2n$ degree system given by equation (10) is

$$\mathbf{E}\dot{\boldsymbol{\xi}} + \mathbf{F}\boldsymbol{\xi} = \mathbf{0}, \tag{13}$$

where

$$\mathbf{E} = \begin{bmatrix} \mathbf{0} & \mathbf{M} \\ \mathbf{M} & \mathbf{C} \end{bmatrix}, \qquad \mathbf{F} = \begin{bmatrix} -\mathbf{M} & \mathbf{0} \\ \mathbf{0} & \mathbf{K} \end{bmatrix}. \tag{14}$$

The eigenvalues and corresponding eigenvectors of equation (13) are represented by λ_1, $\lambda_2, \ldots, \lambda_{4n}$ and $\boldsymbol{\Psi}_1$, $\boldsymbol{\Psi}_2, \ldots, \boldsymbol{\Psi}_{4n}$, where

$$\boldsymbol{\Psi}_i = [\lambda_i \quad \boldsymbol{\phi}_i \quad \boldsymbol{\phi}_i]^{\mathrm{T}}, \tag{15}$$

$i = 1, 2, \ldots, 4n$, $\boldsymbol{\phi}_i$ is the eigenvector of equation (10). Then the solution of equation (10) can be written as

$$\boldsymbol{\eta}(t) = \sum_{i=1}^{4n} \frac{\mathrm{e}^{\lambda_i t}}{a_i} \boldsymbol{\phi}_i \boldsymbol{\phi}_i^{\mathrm{T}} \{\mathbf{M}[\dot{\boldsymbol{\eta}}(0) + \lambda_i \boldsymbol{\eta}(0)] + \mathbf{C}\boldsymbol{\eta}(0)\}, \tag{16}$$

where $a_i = 2\lambda_i \boldsymbol{\phi}_i^{\mathrm{T}} \mathbf{M} \boldsymbol{\phi}_i + \boldsymbol{\phi}_i^{\mathrm{T}} \mathbf{C} \boldsymbol{\phi}_i$. By substituting equation (16) into equation (6), one can obtain the motions of the beam. From equation (16), if the real partition of one of the $4n$ eigenvalues is positive, $\boldsymbol{\eta}(t)$ will increase very fast along with the increase of the time t. Then, the vibrations of the beam show an increase with respect to time instead of decay expected by the original design.

3. NUMERICAL RESULTS AND DISCUSSIONS

Numerical calculations have been carried out for an intelligent beam with given parameters: $l_0 = 400$ mm, $w = 20$ mm, $h_1 = 0{\cdot}3$ mm, $h_2 = 1$ mm, $\rho_1 = 1780$ kg/m^3, $\rho_3 = 8000$ kg/m^3, $Y_1 = 2$ GPa, $Y_2 = 210$ GPa, $d_{31} = 80 \times 10^{-12}$ C/N. Five sets (the cases in Table 1) of specified values for the other parameters are adopted in the calculation. The numerical results of eigenvalues for every case are shown in Table 1 for $n = 8$. In Table 1, for each case there are some eigenvalues whose real parts are positive. Other calculations are also performed for $n = 1, 2, 4$ and 16, for varied material constants, and for a beam with initial damping. The numerical results also give eigenvalues with positive real parts for each calculation. These calculations reflect that the dynamic characteristics of the intelligent beam for the calculations are arbitrary. According to the analysis in section 2, such a beam does not work. As to relevant published experiments, one can only find one conducted by Lee [8]. All other published works only give theoretical and numerical analyses. Lee's experiment [8] investigated the instability of an intelligent beam (referenced by Plate No. 1 in [8]) using a collocated piezoelectric sensor/actuator pair under arbitrary feedback gain. The present analysis gives the exact reason of this instability. In other words, the available experiment corroborates the authors conclusion to some extent. However, Lee explains that this instability comes from the actual factors such as "system non-linearity, electronic signal delay, and low-pass filters in the compensator that add further phase lag to the overall system". Here, these factors are believed to be less important and can influence the stability of the beam only near the critical point between the stable and unstable region. They cannot influence the stability of the beam itself or cannot influence the stability of the beam under arbitrary feedback gain. Hence, Lee's explanation may not be accurate.

Other intelligent flexible structures using the asymmetric piezoelectric sensing/actuation technique have the same dynamic characteristic—the sensor senses both the motions in the directions with higher stiffness of a flexible structure and the motion in the expected direction with lower stiffness; the actuator actuates both the motions in the directions with higher stiffness of a flexible structure and the motion in the expected direction with lower stiffness. Generally, the eigenvalues of the EOMs of the structures also have those with positive real parts. Hence, the asymmetric piezoelectric sensing/actuation technique is not feasible.

In the analysis in section 2, by neglecting the motion of the beam in the longitudinal direction, the EOM of the beam describes a pure velocity negative feedback problem. In this situation, all the corresponding eigenvalues are sure to have no positive real parts. Then, the solution of the transverse motion of the beam decays with respect to time, i.e., the vibration of a structure can be suppressed by this sensor/actuator pair technique. This is a conclusion drawn from the previous analyses which neglect the motions of a structure in its higher stiffness direction. Obviously, it contradicts the above exact analysis.

To overcome the shortcoming of the asymmetric collocated sensor-actuator pair technique, the symmetric collocated sensor/actuator technique (see Figure 3) [16] can be adopted (of course, to do this adds to the complexity of a structure). This technique uses two piezoelectric sensors, located at the two positions that are symmetric with respect to the midplane of a flexible structure, to sense symmetrically the motions of the structure. According to equation (1), it is easy to conceive that the sum of the outputs of the two sensors includes only the information of the motion in the transverse direction, while the information of the motions in the midplane is cancelled. The two actuators are distributed similarly. If the sum of the sensors' output is used as feedback, an the two actuators are subjected to two equal and opposite feedback voltages, only the transverse motion

TABLE 1

The calculated eigenvalues for each case of specified parameter values (the number of the eigenvalues is 32 for each case, the units of l_1 and l_2 is mm)

Cases	Eigenvalues	
$l_1 = 0$	−0·891580 ± 30·953965i, −0·134936 ± 194·103454i, −19·090957 ± 538·948008i,	
$l_2 = 200$	−0·001101 ± 1065·076830i, −39·131712 ± 1728·931418i, 2330·027501 ± 0·000000i,	
$G = 1{\cdot}0 \times 10^9$	−0·000002 ± 2630·104864i, −31·556186 ± 3616·210357i, 0·000000 + 4890·690869i,	
	2126·350292 ± 38896·879818i,	2081·044161 ± 77850·637697i,
	2004·677528 ± 116837·394641i,	1892·015409 ± 155895·448450i,
	1734·197449 ± 195079·852480i,	1512·284959 ± 234503·549466i,
	1172·252765 ± 274508·346055i,	1101573·509040 − 0·000001i
$l_1 = 0$	−1·250883 ± 30·968453i, −14·90973 ± 192·553660i, −35·068851 ± 529·888409i,	
$l_2 = 400$	−45·124762 ± 1026·115858i, 1458·453661 + 0·000000i, −38·249133 ± 1701·365718i,	
$G = 1{\cdot}0 \times 10^9$	−27·327740 ± 2562·470865i, −18·676806 ± 3604·625610i, −12·372581 ± 4824·884016i,	
	1056·458309 ± 38837·120791i,	1034·077793 ± 77786·404202i,
	997·373659 ± 116758·886855i,	943·067658 ± 155803·516650i,
	866·458292 ± 194978·990071i,	757·735725 ± 234401·692944i,
	589·289630 ± 274419·794998i,	2242659·834047 + 0·000001i
$l_1 = 100$	−0·252538 ± 30·981387i, −24·707238 ± 191·004437i, −0·717971 ± 543·325098i,	
$l_2 = 300$	−19·818155 ± 1056·835323i, −0·085378 ± 1760·601017i, −135·042626 ± 2472·861106i,	
$G = 1{\cdot}0 \times 10^9$	2591·016465 + 0·000000i, −0·001936 ± 3673·448273i, −14·374516 ± 4854·288416i,	
	762·088453 ± 25632·636622i,	691·596005 ± 77111·094816i,
	418·816331 ± 128159·558739i,	1586·226928 ± 159679·826128i,
	1239·689384 ± 181642·810965i,	596·908073 ± 232118·434044i,
	154·823465 ± 281695·500268i,	2244346·822822 − 0·000001i
$l_1 = 0$	−0·070691 ± 30·974319i, −1·855996 ± 194·118199i, −9·350185 ± 543·300971i,	
$l_2 = 40$	−20·251430 ± 1063·215941i, −25·811931 ± 1755·750715i, −19·359498 ± 2624·446226i,	
$G = 1{\cdot}0 \times 10^9$	−5·656442 ± 3671·283743i, −0·669716 ± 4890·371353i, 12728·308263 − 0·000000i,	
	1119·985795 ± 20686·241164i,	1387·013624 ± 63771·802275i,
	1349·984284 ± 106560·242047i,	1256·839700 ± 149278·652184i,
	1117·113228 ± 191952·464763i,	923·256692 ± 234567·851464i,
	654·228729 ± 277091·658505i,	1318075·220779 − 0·0000001i
$l_1 = 0$	−0·707028 ± 30·996310i, −18·843607 ± 194·817900i, −91·483513 ± 519·708780i,	
$l_2 = 40$	−108·331503 ± 959·373233i, −57·720692 ± 1650·120372i, 1762·524341 ± 0·000000i,	
$G = 1{\cdot}0 \times 10^{10}$	−22·327397 ± 2565·526893i, −4·155276 ± 3657·584201i, −0·346212 ± 4889·039832i,	
	142·539230 ± 21311·600531i,	140·915864 ± 63985·973392i,
	134·858251 ± 106646·662842i,	125·213213 ± 149297·712260i,
	111·417221 ± 191929·707903i,	92·365346 ± 234521·276058i,
	65·749301 ± 277040·581044i,	13459762·401896 + 0·000002i

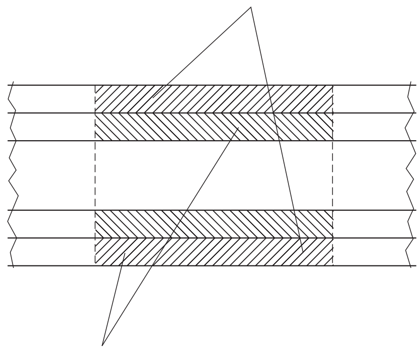

Figure 3. The symmetric collocated sensing/actuation technique that uses two sensors and two actuators.

is involved in the closed-loop EOM of structure for the pure bending actuation effect of the two actuators. In this situation, one can consider only the motion in the transverse direction. Then, the problem also becomes a pure velocity negative feedback problem. In principle, the problem is absolutely stable, and the vibration of the structure can be suppressed.

If the intelligent beam does not use the piezoelectric sensor as its sensor, and other sensing techniques, such as attaching a mini accelerometer on the top or bottom surface of the beam as a sensor to measure the transverse velocity of the beam, are adopted (to to this also adds to the complexity of the beam) to sense only the transverse motion of the beam, and the piezoelectric actuator of the beam is kept unchanged, the conclusion is opposite. In this situation, the EOM of the beam can also be written as the form of equation (8) when the mass of the mini accelerometer is neglected. The change is only made on the coefficients. If the mini accelerometer is attached to the free end of the beam, the coefficients are changed as: $b_1 = 0$, $b_3 = 0$ and $c_{3i} = U_{3i}(l_0) - U_{3i}(0)$, $i = 1, 2, 3, \ldots$. The numerical results show none of the eigenvalues have positive real parts. That is, in this situation the intelligent beam does work. For example, the calculated eigenvalues for the case of $l_1 = 0$, $l_2 = l_0$, $G = 5 \times 10^8$ and $n = 4$ are: $-0{\cdot}016250$, $-0{\cdot}078590 \pm 136{\cdot}242542i$, $-0{\cdot}257673 \pm 444{\cdot}838066i$, $-0{\cdot}455861 \pm 940{\cdot}701378i$, $\pm 18951{\cdot}827157i$, $\pm 56855{\cdot}481470i$, $\pm 94759{\cdot}135783i$, $\pm 132662{\cdot}790097i$, $-229374{\cdot}976853$. The experiment done by Tzou and Gadre [9] also confirmed that such a sensing/actuation technique can suppress the vibration of a beam.

4. CLOSURE

A new method has been proposed for direct and analytical analysis of the motion of a flexible structure using distributed piezoelectric sensors/actuators to sense and control its vibration. Exact numerical calculations conclude that an intelligent beam using the collocated piezpelectric sensor/actuator pair technique is not feasible. This conclusion is opposite from the corresponding previous one that is concluded from the approximate analysis (neglecting the undesired motions in the directions associated with higher stiffness of a structure). Experiment phenomena support this new conclusion. The same conclusion can be applied to other flexible structures using the asymmetric piezoelectric sensing/actuation technique. The unfeasibility comes directly from the closed-loop dynamic characteristic of a structure, which generally does not guarantee the stability of the structure for the asymmetric sensing and actuation situation. The other two feasible sensing/actuation techniques have also been discussed.

REFERENCES

1. T. Bailey and J. E. Hubbard 1985 *Journal of Guidance, Control, and Dynamics* **8**, 605–611. Distributed piezoelectric-polymer active vibration control of a cantilever beam.
2. S. S. Rao and M. Sunar, 1994 *Applied Mechanics Review* **47**, 113–123. Piezoelectricity and its use in disturbance sensing and control of flexible structures: a survey.
3. M. Sunar and S. S. Rao, 1997 *American Institute of Aeronautics and Astronautics Journal* **35**, 534–539. Thermopiezoelectric control design and actuator placement.
4. H. S. Tzou, 1992 *Journal of Sound and Vibration* **153**, 335–349. A new distributed sensor and actuator theory for "intelligent" shells.
5. W.-S. Hwang and H.-C. Park 1993 *American Institute of Aeronautics and Astronautics Journal* **31**, 930–937. Finite element modeling of piezoelectric sensors and actuators.
6. C.-Q. Chen, X.-M. Wang and Y.-P. Shen 1996 *Computers and Structures* **60**, 505–512. Finite element approach of vibration control using self-sensing piezoelectric actuators.
7. C. K. Lee 1990 *Journal of the Acoustical Society of America* **87**, 1144–1158. Theory of laminated piezoelectric plates for the design of distributed sensors/actuators. Part I: governing equations and reciprocal relationships.
8. C. K. Lee, W. W. Chiang and T. C. O'Sullivan 1991 *Journal of the Acoustical Society of America* **90**, 374–384. Piezoelectric modal sensor/actuator pairs for critical active damping vibration control.
9. H. S. Tzou and M. Gadre 1989 *Journal of Sound and Vibration* **132**, 433–450. Theoretical analysis of a multi-layered thin shell coupled with piezoelectric shell actuators for distributed vibration controls.
10. S. E. Miller, Y. Oshman and H. Abramovich 1996 *American Institute of Aeronautics and Astronautics Journal* **34**, 1868–1875. Modal control of piezoelectric anisotropic rectangular plates. Part I: modal transducer theory.
11. D. C. Sun, D. Wang and Z. L. Xu, 1997 *American Institute of Aeronautics and Astronautics Journal* **35**, 583–584. Distributed piezoelectric segment method for vibration control of smart beams.
12. L. Yin, X.-M. Wang and Y.-P. Shen 1996 *China Journal of Vibration Engineering* **9**, 107–115. The numerical analysis of vibration control of composite laminates by piezoelectric devices.
13. C. P. Smyser and K. Chandrashekhara, 1997 *Smart Materials and Structures* **6**, 178–189. Robust vibration control of composite beams using piezoelectric devices and neural networks.
14. T. Ikeda 1990 *Fundamentals of Piezoelectricity*. Oxford: Oxford University Press.
15. Z. H. Li 1989 *Vibration Mechanics*. Xian, China: Xian Jiaotong University Press.
16. B. T. Wang and C. A. Rogers 1991 *Journal of Composite Materials* **25**, 433–452. Laminated plate theory for spatially distributed induced strain actuators.